UCRL- 91625
PREPRINT

HIGH-ENERGY AIR SHOCK STUDY IN A GROUT PIPE

H. D. Glenn
D. D. Keough
H. R. Kratz
D. A. Duganne
D. J. Ruffner
D. Baum

This paper was prepared for presentation at the 15th International Symposium on Shock Waves and Shock Tubes, July 28-Aug. 2, 1985, Berkeley, CA.

June, 1985

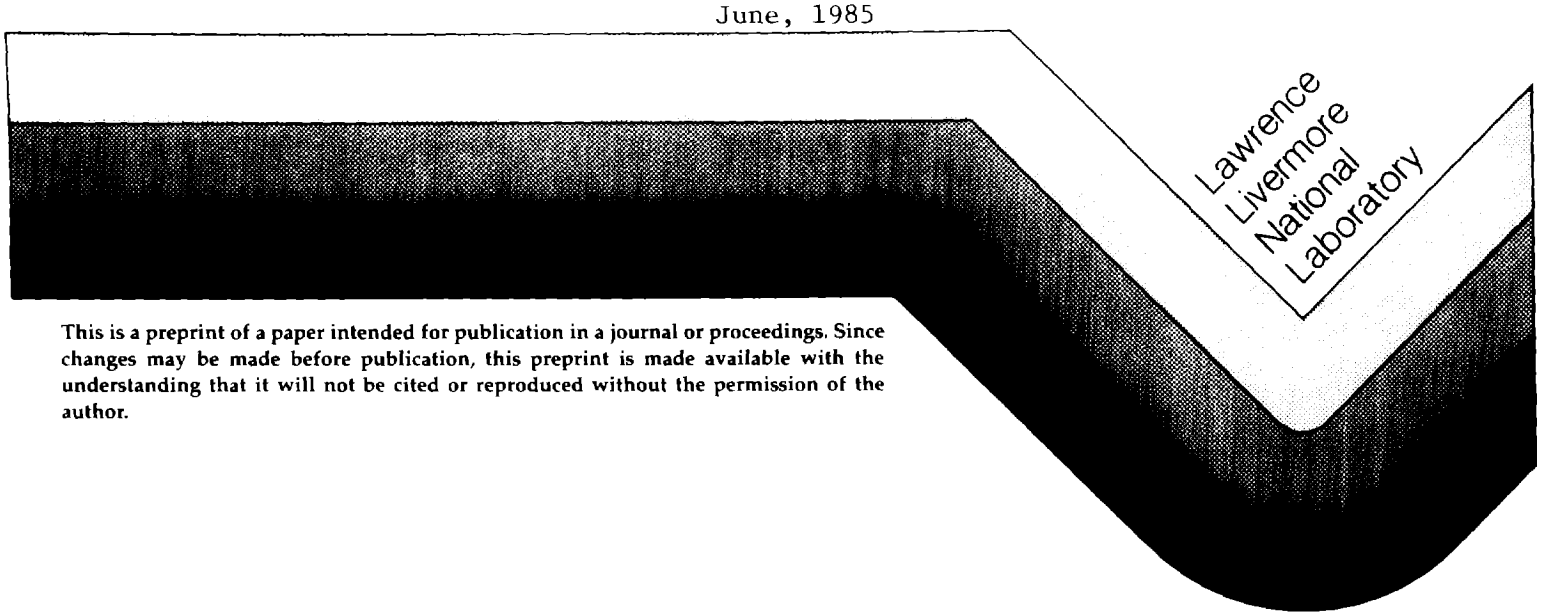

HIGH-ENERGY AIR SHOCK STUDY IN A GROUT PIPE

H. D. Glenn, D. D. Keough,* H.R. Kratz,**
D. A. Duganne, D. J. Ruffner, and D. Baum†

Lawrence Livermore National Laboratory,Livermore, CA 94550
*SRI International, Menlo Park, CA 94025
**Systems, Science and Software, LaJolla, CA 92037
†Artec Associates, Hayward, CA 94545

A modified Voitenko compressor generated a 43 mm/μs air shock in a 20-mm-i.d. 3.0 m. long pipe containing ambient atmospheric air. The first 0.15 m of outlet pipe was constructed of steel and the last 2.85 m of DR-1 grout. Between 0.10- and 2.5-m from the diaphragm the velocity of the shock front attenuated from 43- to 4.5-mm/μs and peak pressure from 2.28- to 0.024 GPa. The rate of wall expansion uniformly decreases and asymptotically approaches an apparent final radius between 60-100 μs behind the shock front. Plasma flow measurements indicated a flow velocity of 27.4 mm/μs and a magnetic Reynolds number >60. Wall expansion was <1 mm at the end of the pipe indicating significant attenuation of the shock front between 2.5 m and 3.0 m.

INTRODUCTION

For nearly two decades the Voitenko generator[1] has been used to study high-energy air-shock and gas-jet propagation. Early Voitenko studies[1,2] used outlet pipes with walls of transparent material. High gas pressures resulted in massive venting and limited optical studies to conditions in or just behind the air shock or gas jet front. The use of steel walls[3] for the outlet pipe virtually eliminated venting and fiber optic ports significantly extended the period for optical measurements (e.g. brightness temperature[4]). The steel walls also provided the rigid mechanical support for installation of other diagnostic sensors[3] (e.g., sigma pins, pressure gages).

This paper describes an experiment that used a modified Voitenko compressor[2,3] to study air-shock propagation in a 3 m long outlet pipe. Some of the hardware and diagnostics coverage are common to an earlier experiment using a steel outlet pipe.[5] For example, the high-explosive (HE) assembly, compressor section, and the first 0.15 m of the outlet pipe are identical within tight machine tolerances. The last 2.85 m of outlet pipe, with its walls of DR-1 grout, allowed use of diagnostics (flat-pack, wall motion, and plasma flow gages) for the first time since their use would not have been feasible in earlier experiments with outlet pipes of glass or steel. Optical and pressure measurements along the first 0.15 m of outlet pipe provided assurance that the initial air shock and plasma flow conditions were similar to previous experiments.

Figure 1 and Table 1 summarize the physical features and diagnostics for the compressor outlet pipe. The detonated HE drives the stainless-steel plate into the chamber, compressing the 1.066-MPa air (initially in the chamber) to high pressures (>100 GPa), densities (>1.0 Mg/m^3), and temperatures (>10 eV) before the diaphragm breaks.[6,7] Expansion of this compressed air down the exit pipe generates a high velocity (Mach 130) air shock. Fiber-optic ports provided optical records are then reduced to give time-of-arrival (TOA) information about air-shock propagation down the outlet pipe. Bar[8] and flat-pack[9] gages provided pressure profiles at numerous locations and the

radial wall motion induced by the high pressures was monitored with mutual inductance particle-velocity gages.[10] Finally plasma flow velocity and conductivity measurements[11] were obtained in the grouted segment of the outlet pipe.

2.0 GROUT SHOCK-TUBE ASSEMBLY

Problems and complexity of the grout shock tube construction added considerably to the effort and expense. Accommodation of the extensive diagnostics required the grout shock tube to be assembled in stages. A cylindrical steel frame was built and four DR-1 grout disks 19 mm thick, 152 mm o.d., with a 20 mm hole in the center, were installed in the center of the frame at specific locations. The grout disks eliminated any effect of the steel frame on wall motion induced by pressures in the plasma flow during the experimental times of interest. A 3-m-long, 19-mm o.d., 0.9-mm-thick copper tube covered with a 0.5 mm-thick heat-shrink plastic tube was inserted through the four disks. This 20-mm-o.d. copper and plastic tube, or bore tube, provided the form for the the 20 mm bore through the grout section of the shock tube.

The plasma flow velocity sensors, conductivity sensors, and the flat-pack gages were attached to the steel frame. The steel frame was then inserted into a 0.508-m-o.d. steel pipe. Fiber optics, bar and wall motion gages were inserted through ports in the steel pipe until contact was made with the bore tube. End plates were mounted and all ports (sensor, alignment, and cable exit) were sealed with epoxy. To remove air entrained in the grout the grout was mixed at reduced pressure in a large tank and added to the steel pipe after it had been evacuated with a roughing pump. Preliminary tests indicated that entrained air tended to migrate to the nearest surface and collect as small air pockets of up to 1 mm in diameter. A large number of air pockets along the bore wall would have a significant but indeterminate effect on the plasma flow. A week prior to the shot date a 0.33 N solution of nitric acid was circulated for 16 h through the bore tube to dissolve the copper tubing. The heat-shrink tubing was left in place to prevent drying of the surface of the 20 mm grout bore and removed shortly before the shot. Visual inspection of the 20 mm bore indicated a smooth wall along its entire length.

3.0 OPTICAL AND ELECTRONIC DIAGNOSTIC COVERAGE

Two framing cameras were focused on the first 0.20 m of the steel-grout outlet pipe to detect the location and duration of possible venting. Of particular interest were the bar gage at 0.10 m and the junction between the steel pipe and grout pipe at 0.15 m. Four of the light pipes were located in the 0.15 m section of steel outlet pipe and the other 11 light pipes were located in the grout section (Table 1). The other end of the light pipes were terminated in an optics display board for scanning by streaking cameras.

The input ends of the first eight bar gages were machined to a 10-mm radius to conform to the curvature of the bore radius. The end of the stagnation bar gage at 3.0 m was flush with the end wall. The seven flat-pack gages were installed in the grout section with the center of the piezoresistance elements at the same axial location as the bar gages. The flat-pack gages were initially developed[9] to monitor high-energy gas flows comparable to those in the present experiment. Radial wall motion was monitored using a mutual-inductance particle velocity gage[10] at seven different axial locations. Each gage consisted of a closely wound primary and secondary conducting wires forming two rectangle loops with lengths large compared to the lateral dimensions. Radial motion of the walls results in alteration of mutual inductance between loops and can be related to wall motion. Plasma

flow velocity, plasma resistance, and plasma electrical conductivity measurements were made at 367, 427, and 735 mm from the diaphragm. Reference 11 gives details of the theory, diagnostics sensors, calibration procedures and previous experimental results.

4.0 EXPERIMENTAL RESULTS

The optical and electronic measurements were correlated in time by reference to the electronic signal used to initiate detonation of the plane-wave lens. The time interval between detonation of the plane-wave lens and diaphragm breakage was 57.6 μs. This time was determined with a light pipe oriented to view the center of the diaphragm and the streaking camera focused on the display board. The diaphragm breaking time is taken as the new zero time reference for all experimental results in this test.

4.1 Optical and TOA Results

The framing camera provided photographic evidence that a small amount of venting around the bar gages at 0.10 m began at 25 μs after the diaphragm broke. Venting continued until high-explosive gases from the driver section obscured the field of view approximately 20 μs later. Venting after 25 μs should have negligible influence on propagation of the shock front.

Table 1 summarizes TOA results for the shock front. The TOA values for the fiber optics are the times that the first luminosity peak was recorded at each location. The TOA values for the bar and flat-pack gages are the times when the rate of pressure increase was the greatest for the first pressure peak. This time was chosen instead of the peak pressure since the peak pressure was delayed by dispersion for the bar gage and time for the shock to travel the length of the piezoresistant grid for the flat-pack gages. A similar criterion was applied to the TOA values for the wall motion gages. Figures 2 and 3 show TOA and velocity plots, respectively, for propagation of the shock front in the exit pipe. After a short period of acceleration the shock attains a maximum velocity of 43 mm/μs at a distance of 0.10 m from the diaphragm. The velocity of the shock front attenuated from 43 to 4.5 mm/μs between 0.10 and 2.5 m. The only other documented study in the open literature using a grout type wall material was the Marvel experiment.[12] That study identified the delayed entrainment of wall material as the principal mechanism for attenuation of the shock front.

4.2 Pressure Profiles

Figures 4-11 give pressure profiles obtained for this experiment. Peak pressures in the shock front decayed from 2.28 GPa at 0.10 m to 0.024 GPa at 2.5 m from the diaphragm. For locations where bar and flat-pack gages can be compared there appears to be agreement in timing and amplitudes of the first two peaks. Generally the pressure oscillations of the flat-packs are larger and probably more indicative of the pressures exerted at the walls. Dispersion in the input bar of the bar gage tends to broaden the pressure pulse and lower the peak pressure arriving at the quartz crystal. The observed pressure oscillations result from axial and radial oscillations of the flow induced by early diaphragm break[13] and radial convergence of driver gas in the compressor chamber.[7] The fact that the oscillations persist over a substantial distance supports the argument of delayed entrainment of wall material.

4.3 Radial Wall Motion

Figure 12 gives radial displacements vs time where the time axis for each radial displacement shown has been shifted so that zero time corresponds to TOA of the shock front (Table 1) at the respective wall motion gage. The initial rapid wall expansion is consistent with the high pressures immediately behind the shock front. Most of the radial expansion appears complete by 60 μs when pressures behind the shock front are greatly reduced. Postshot the grout section beyond 0.8 m was recovered intact. The final bore diameter at 0.8 m measured 60 mm, corresponding to a radial expansion of 20 mm. Wall motion measurements of radial expansion at 100 μs behind the shock front at 0.50 and 1.00 m were 19 and 4.6 mm, respectively. If these values are reasonably accurate, then appreciable radial wall motion occurred after 100 μs. Postshot measurement of the bore diameter at 3.0 m indicated <1 mm radial expansion. Consequently, significant attenuation occurred between 2.5 and 3.0 m since measurements at 2.5 m indicated a shock propagating at 4.5 mm/μs.

4.4 Plasma Flow Velocity and Conductivity Measurements

Figure 13(a) illustrates the time history for the plasma flow velocity from an analysis of the velocity gage record at 367 mm from the diaphragm. Figure 13(b) shows the plasma effective conductivity vs time results from the load voltage and load current measurements. The conductivity measurements resulted in a magnetic Reynolds number >60 requiring correction to the velocity and plasma-resistance results. Corrections based on the eddy current effects are shown as the dashed line in Fig. 13(a) and have already been incorporated in the conductivity history of Fig. 13(b). At 367 m the shock velocity (U) was measured at $\sim$ 32 mm/μs (Fig. 3). The plasma flow velocity (u) can be obtained from the measured shock speed using the relation $u = 2\,U/(\gamma+1)$, where γ is the gas equation of state parameter. Using $\gamma = 1.208$ for air gives $u = 29.0$ mm/μs, which is in good agreement with the corrected measured initial flow velocity of 27.4 mm/μs. For a more detailed discussion of the diagnostics and experimental results than is presented in this paper the reader is referred to reference 13.

ACKNOWLEDGMENTS

Work performed under the auspices of the U.S. Department of Energy by the Lawrence Livermore National Laboratory under contract number W-7405-ENG-48 and Defense Nuclear Agency Subtask J24AAXIX955. The authors are indebted to G. W. Ullrich for his council and support throughout the program, and to C. Knowles, B. Hartenbaum, B. K. Killian, K. Pyatt, and H. L. Brode for their advice. The authors are grateful to N. W. Stewart for mechanical assembly, C. H. Dittmore for film processing, A. M. Ban for drafting support, L. F. Simmons and the 850 bunker crew for their high quality field support, J. B. Bryan and R.P Swift for their critical review of this paper, R. M. Glenn and L. D. Grabowski for report preparations.

REFERENCES

1. Voitenko, A.E., "Generation of High Speed Jets," Sov. Phys. Dokl. Vol. 9, 1966, p. 860.
2. Sawle, D., "Characteristics of the Voitenko High Explosive Driven Gas Compressor," First Intern. Colloq. of Gas Dynamics of Explosions, Brussels (18-21 Sept. 1967).
3. Glenn, H.D.,and Crowley, B.K., "Optical Technique for Monitoring High Energy (Mach 34-130) Shocks in Steel Pipes Containing Ambient Atmospheric Air," LLNL Report UCRL-71007 April 1968.

4. Glenn, H.D., "High Energy Oxygen Jet Propagation," J. Appl. Phys. Vol. 44, June 1973, p. 2585.
5. Glenn, H.D., Kratz, H.R., Keough, D.D., and Swift, R.P., "High-Energy Air Shock Study in Steel Pipe," Proc. 13th Intern. Symp. Shock Tubes and Waves, Niagara Falls, NY, 6-9 July 1981, p. 191.
6. Crowley, B.K., and Glenn, H.D., "Numerical Simulation of a High Energy (Mach 120 to 40) Air Shock Experiment," Proc. 7th Intern. Shock Tube Symp., Toronto, Canada, 23-25 June 1969, p. 314.
7. Brown, P.S., and Lohmann, M.L., "Computer Modeling of the Voitenko Tube Generator," in Proc. Sixth Intern. Symp. on Military Applications of Blast Simulations, Cahors, France, 25-29 June 1979.
8. Hartenbaum, B., "A Piezoelectric Transducer for Measuring Sub-Millisecond Pressure Pulses with Amplitudes up to 30 Kilobars," Gulf General Atomic Report GAMD-8474, 1968.
9. Glenn, H.D., "Diagnostics Techniques Improvement Program," Defense Nuclear Agency Report, Systems, Science and Software, DNA 2978T, 1972.
10. Danek, W.L., Shooley, D.J., and Jerogal, F.A., "Particle Velocimeter for Use Close in to Underground Explosions," Engineering Physics Co., Report, DASA-1431-3, 1967.
11. Gill, S.P., Mukherjee, D., and Baum, D.W., "MHD Velocity Gage Study," Artec Associates Inc., Final Report 128, 1979.
12. Crowley, B.K., Glenn, H.D., and Marks, R.E., "An Analysis of Marvel - A Nuclear Shock Tube Experiment," J. Geophys. Res. Vol. 76, May 1971, p. 3351.
13. Glenn, H.D., Kratz, H.R., Keough, D.D., Duganne, D.A., Ruffner, D.J., Swift, R.P., and Baum, D., "High-Energy Air Shock Study in Steel and Grout Pipes," LLNL Report, UCRL-52826, 1979.

Table 1. Diagnostics used and air shock time-of-arrival (TOA) data.

Axial Distance (m)	Diagnostics[a]	Fiber Optics TOA (μs)	Bar Gage TOA (μs)	Flat Pack TOA (μs)	Wall Motion Gage TOA (μs)
0	F	0.0			
0.02	F	1.3			
0.05	F	2.13			
0.10	F, B	3.45	3.9		
0.20	F, B, PM, W	5.74	6.6	6.5	5.6
0.30	F, B, PM, W	8.6	9.6	9.8	9.4
0.40	F	11.4			
0.50	F, B, PY, W	14.6	13.3	14.2	13.4
0.75	F	22.9			
1.00	F, B, PY, W	31.8	32.5	32.8	32.6
1.25	F	43.0			
1.50	F, B, PY, W	57.4	57.4	57.5	56.8
1.75	F	76.9			
2.00	F, B, PY, W	107.7	108.6	108.4	107.4
2.50	F, B, PY, W	208.0	209.3	193.4	
3.00	B				

[a]F = fiber optics; B = bar gage (SSS); PM = pressure - Manganin (SRI); PY = pressure - ytterbium (SRI); W = wall-motion sensor (particle velocity loop) (SRI).

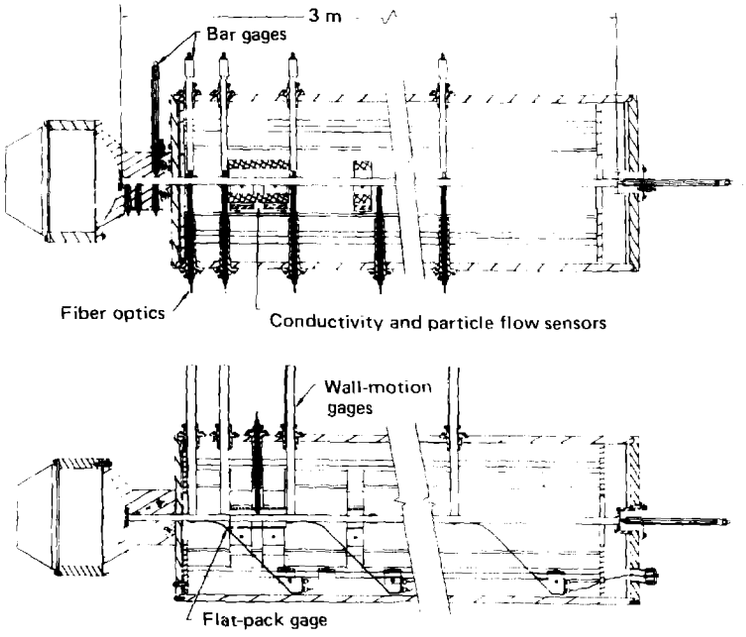

Fig. 1. Compressor, grout pipe and diagnostics.

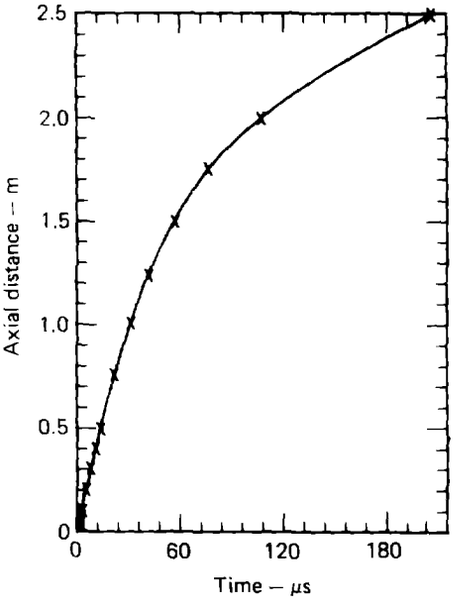

Fig. 2. Air shock TOA.

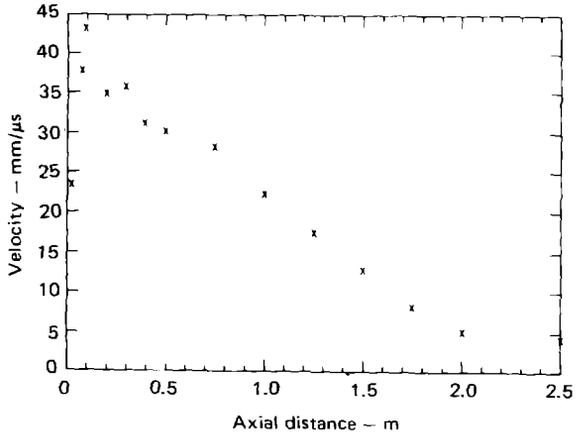

Fig. 3. Shock velocity vs axial distance.

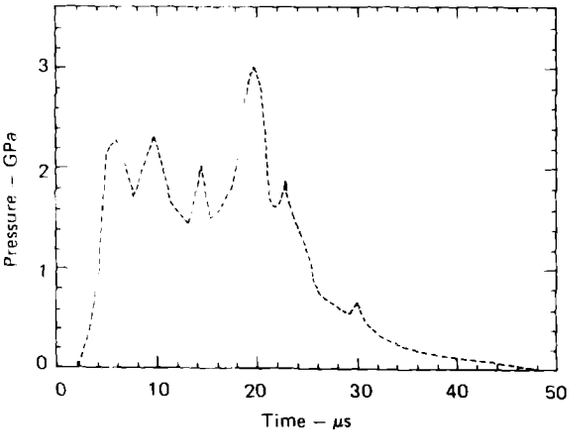

Fig. 4. Pressure history at 0.10 m.

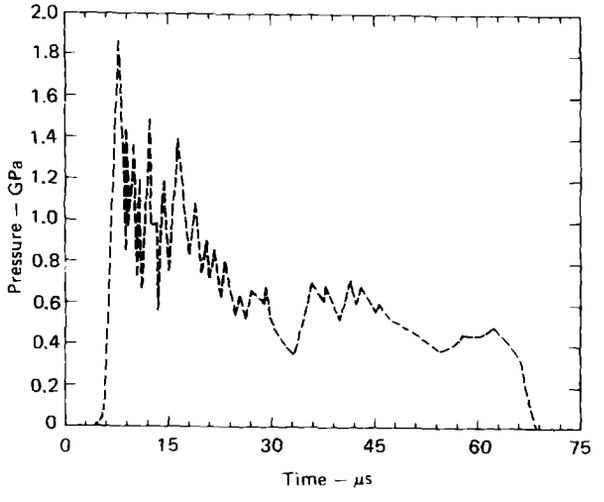

Fig. 5. Pressure history at 0.20 m.

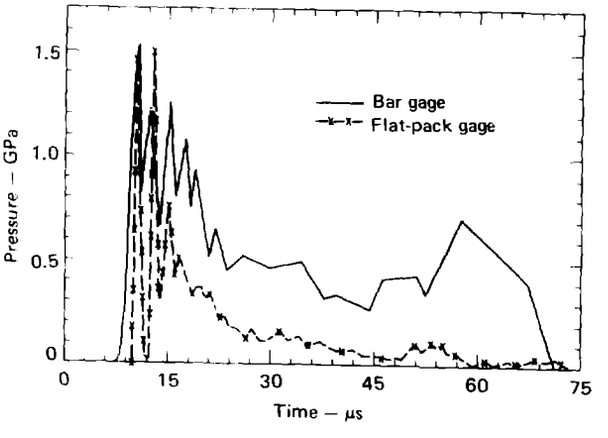

Fig. 6. Pressure history at 0.30 m.

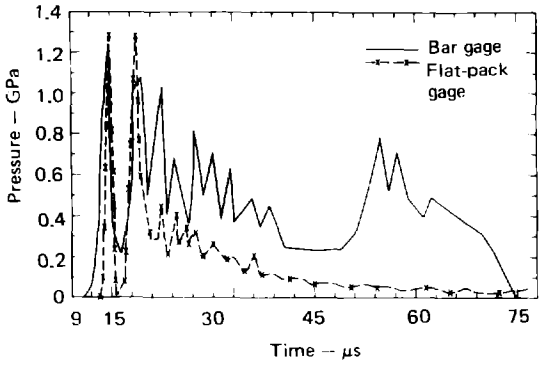

Fig. 7. Pressure history at 0.50 m.

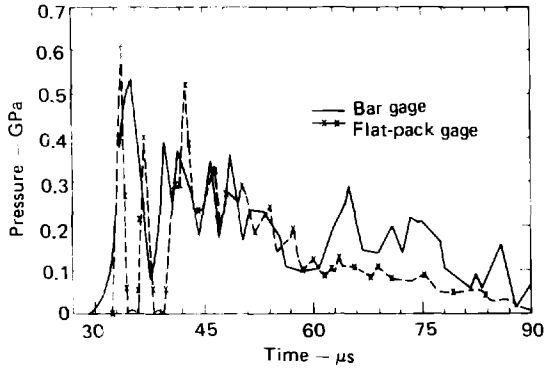

Fig. 8. Pressure history at 1.0 m.

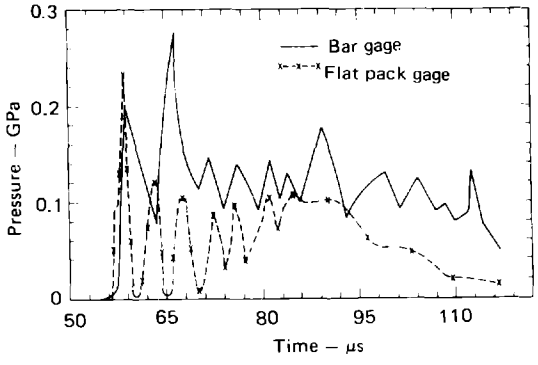

Fig. 9. Pressure history at 1.5 m.

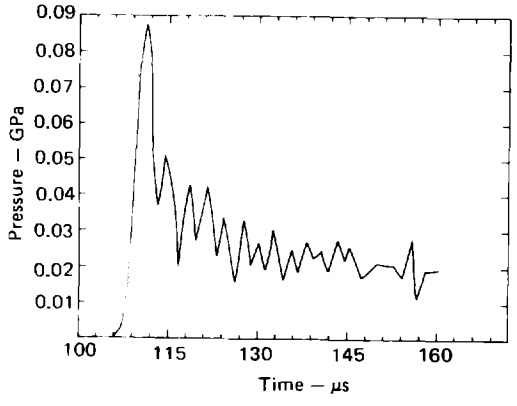

Fig. 10. Pressure history at 2.0 m.

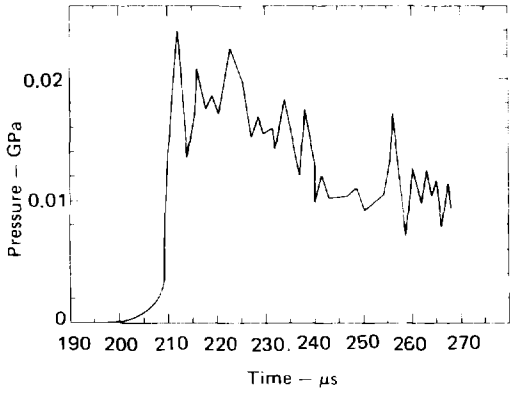

Fig. 11. Pressure history at 2.5 m.

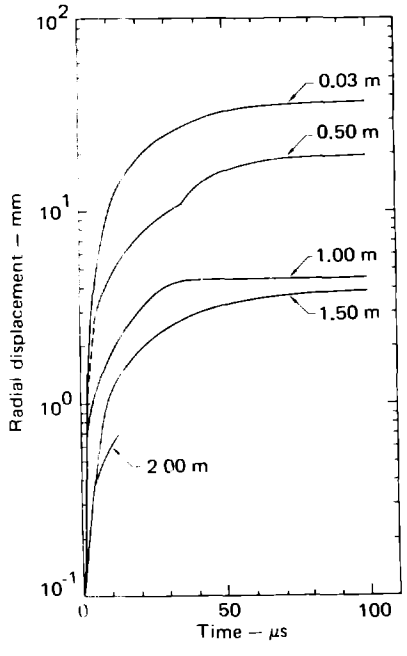

Fig. 12. Wall motion at 0.03, 0.50, 1.00, 1.50 and 2.00 m

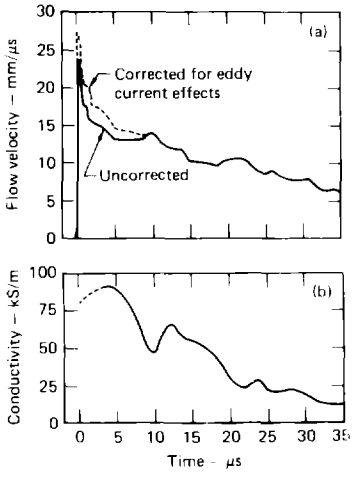

Fig. 13. (a) Plasma flow velocity vs time at 367 mm; (b) plasma effective conductivity vs. time at 427 mm.